

Supplementary Information for ultra-broadband unidirectional launching of surface plasmon polaritons by a double-slit structure beyond the diffraction limit

Jianjun Chen^{1,2*}, Chengwei Sun^{1,2}, Hongyun Li¹, and Qihuang Gong^{1,2*}

¹State Key Laboratory for Mesoscopic Physics and Department of Physics, Peking University, Beijing 100871, China

²Collaborative Innovation Center of Quantum Matter, Beijing, China

*Corresponding author: jjchern@pku.edu.cn and qhong@pku.edu.cn

1. Intensities of the SPPs generated by a single nano-slit

A single nano-slit on a 500-nm-thick gold film is illuminated by a bulky p-polarized beam of $\lambda=830$ nm from the back side. The generated SPP intensities along the front metal surface for different slit widths are investigated with Comsol Multiphysics, and the results are displayed in Figure S1. The single nano-slit can launch two SPPs with equal intensity propagating to the opposite directions on the front metal surface. The SPP intensities generated by the single nano-slit first increase with the slit width and then decrease, as shown in Figure S1. Hence, equal intensities of the generated SPPs can be obtained by using different slit widths.

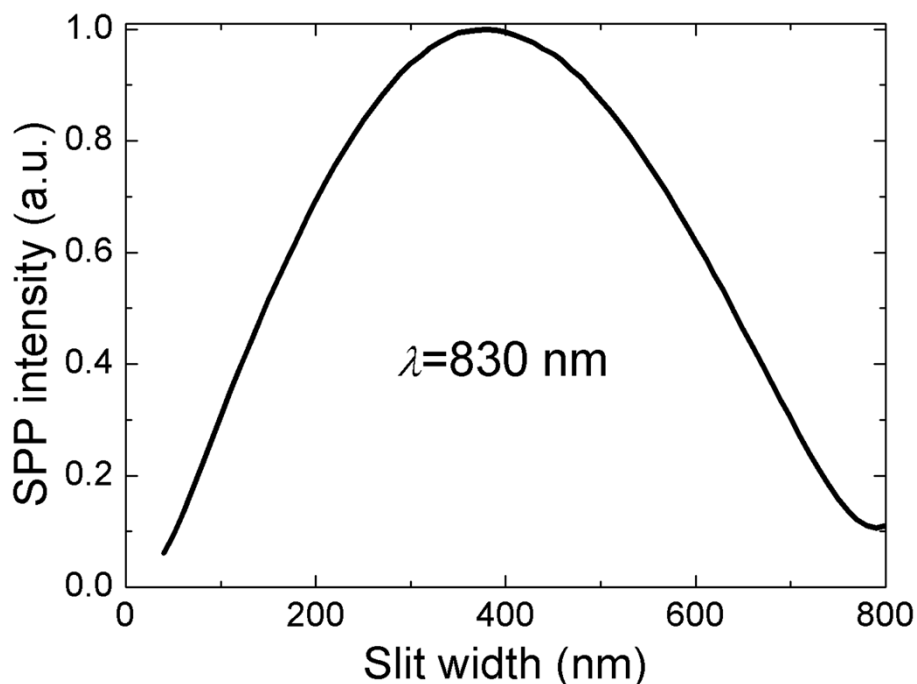


Figure S1. Intensity of the SPPs generated by a single nano-slit for different slit widths at $\lambda=830$ nm.

2. Amplitude of the magnetic field as one slit being illuminated

In the submicron double-slit structure, the amplitude of the magnetic field is calculated at different incident wavelength when only one slit is illuminated, and the results are displayed in Figure S2. For the left direction, the amplitudes of the magnetic field of the SPPs coming from the slit 1 are always greater than that of the SPPs coming from slit 2 [Figure S2(a)]. Thus, the completely destructive interference cannot be obtained in the left direction. This indicates the SPPs in the left direction always exist in the investigated wavelength range [black line in Fig. 2(a)]. For the right direction, the amplitudes of the magnetic fields of the interfering SPPs coming from the slit 1 and the slit 2 are comparable. Considering that the phase difference of $\Delta\Phi_R$ is nearly equal to π in the investigated wavelength range [Fig. 2(b)], almost completely destructive interference can occur for the right direction in investigated wavelength range. This leads to the SPPs in the right direction being very weak [red line in Fig. 2(a)]. Therefore, the SPPs generated by the submicron double-slit structure mainly propagate to the left direction [Fig. 2(a)], resulting in an ultra-broadband unidirectional SPP launcher.

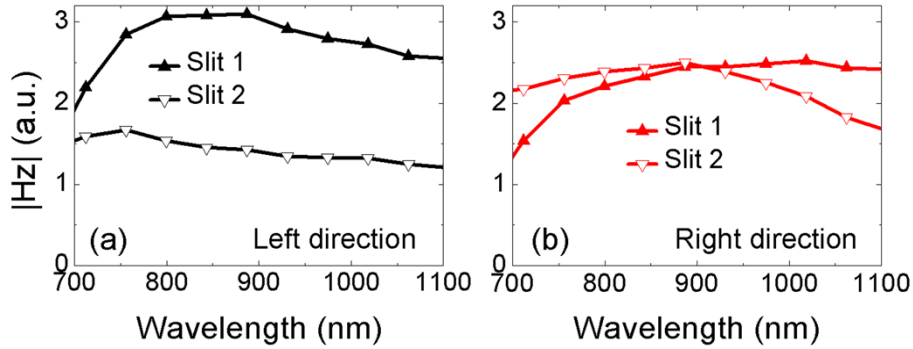


Figure S2. Amplitude analysis as one slit being illuminated in the double-slit structure. Amplitude of the magnetic field at different wavelengths in the (a) left and (b) right directions when only one slit is illuminated in the submicron double-slit structure of $w_1=600$ nm and $w_2=140$ nm.

3. Downscaling unidirectional SPP launcher to be $<\lambda^2/10$

The slit length of the double slit structure can be further downscaled, such as $L_{\text{slit}}=70$ nm. In this case, the metal strip has a cross-section dimension of 70×300 nm² on the 200-nm-thick gold film. The inset in Figure S3(a) displays the field distribution of the SPP mode in the plasmonic waveguide, revealing a subwavelength confinement of the SPPs (mode size of about 200 nm) by the subwavelength metal ridge. The field distribution of the SPPs in the launcher is displayed in Figure S3(a). The unidirectional SPP launching is still observed, and the extinction ratio is about 6 dB. By optimizing the structural parameters, the extinction ratio is increased to 14 dB, as shown in Figure S3(b). Therefore, the occupied area of the unidirectional SPP

launcher can be downscaled to be $0.067 \mu\text{m}^2$, which is smaller than $\lambda^2/10$.

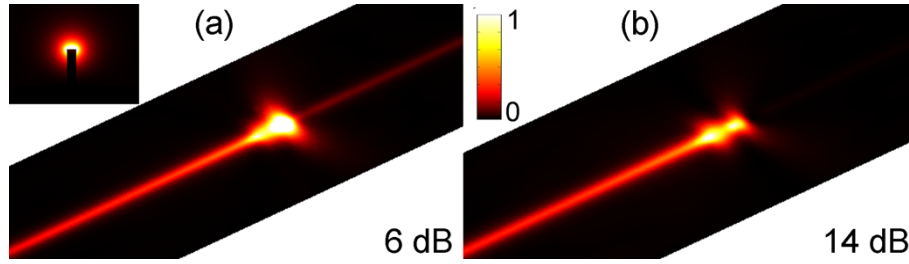


Figure S3. Field distributions. (a) Field distribution (power flow) of the shortened double-slit structure (100 nm above the plasmonic waveguide) at $\lambda=830$ nm when the slit length is downscaled to $L=70$ nm. Inset shows the field distribution of the SPP mode supported by the subwavelength plasmonic waveguide, where $s=L_{\text{slit}}=70$ nm and $h=300$ nm. The SPP mode has an effective refractive index of $n_{\text{eff}}\approx 1.07$, a propagation length of $L_{\text{SPP}}\approx 10 \mu\text{m}$, and a mode size of $D\approx 200$ nm. (b) Field distribution (power flow) of the shortened double-slit structure (100 nm above the plasmonic waveguide) at $\lambda=830$ nm when the structural dimensions of the launcher is optimized to be $w_1=540$ nm, $w_2=120$ nm, and $d=300$ nm.

4. Demonstration of broadband unidirectional SPP launching with a white beam

To intuitively observe the broadband unidirectional SPP launching, the double-slit structure with a subwavelength plasmonic waveguide [Fig. 4(c)] is illuminated by a white beam (wavelengths ranging from about 400 nm to 2400 nm) from the back side, and the obtained CCD picture is displayed in Figure S4. Herein, the response of the CCD becomes very weak when the incident wavelength is greater than 1000 nm. In Figure S4, a bright spot is observed in the left decoupling grating, while a very weak spot is observed in the right decoupling grating. This is a straightforward evidence of that the generated SPPs are mainly coupled to the left plasmonic waveguide for a broad bandwidth, leading to ultra-broadband and ultra-smaller SPP launcher. Moreover, the sizes of the bright spot are much smaller than that of the decoupling gratings, as shown by the red dashed rectangles in Figure S4. So, the ultra-smaller SPP launcher can act as a strongly localized guided SPP source.

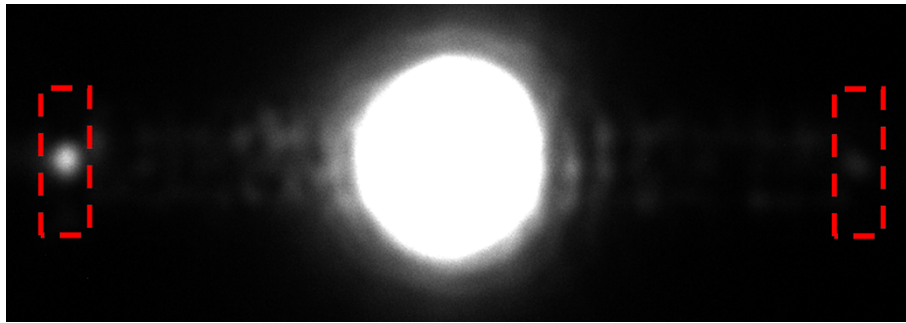


Figure S4. White beam illumination. CCD picture of the scattered light from the experimental sample in Fig. 4(c) when it is illuminated by a white beam. The red dashed rectangles indicate the decoupling gratings.

5. On-chip reference structure

To eliminate the laser power fluctuation and the dependence of the detector sensitivity on the wavelengths in the experiment, an on-chip reference structure is also fabricated. Its SEM image is displayed in Figure S5, which only comprises a single slit in the middle of the subwavelength plasmonic waveguide. The measured width and length of the single slit are about $w=550$ nm and $L=280$ nm, respectively. When a p-polarized incident beam illuminates the referenced structure from the back side, two bright spots with nearly equal intensities are observed at the two decoupling gratings in the CCD pictures, as shown by the top part in Fig. 4(e).

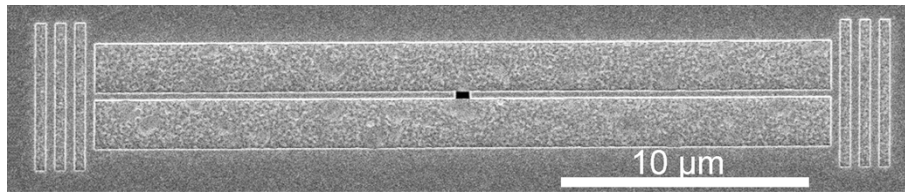


Figure S5. SEM image of the on-chip reference structure. The on-chip reference structure only comprises a single slit in the middle of the subwavelength plasmonic waveguide. The two decoupling gratings on both sides are used to scatter the guided SPPs.

6. Diverging SPP source without coupling plasmonic waveguides

To demonstrate the shortened double-slit structure, which is directly coupled with a subwavelength plasmonic waveguide [Fig. 4(c)], is a strongly localized guided SPP source, a single slit without any coupling plasmonic waveguides is fabricated on the metal surface, as shown in Figure S6(a). When a p-polarized incident beam illuminates the structure from the back side, it is observed that the two whole decoupling gratings are lit up by the generated SPPs, as shown by the CCD picture in Figure S6(b). Obviously, the sizes of the bright spot at the decoupling gratings in Figure S6(b) are much larger than that in Fig. 4(e) and Figure S3. This provides a powerful evidence of that the shortened double-slit structure directly coupled with a plasmonic waveguide is a strongly localized guided SPP source.

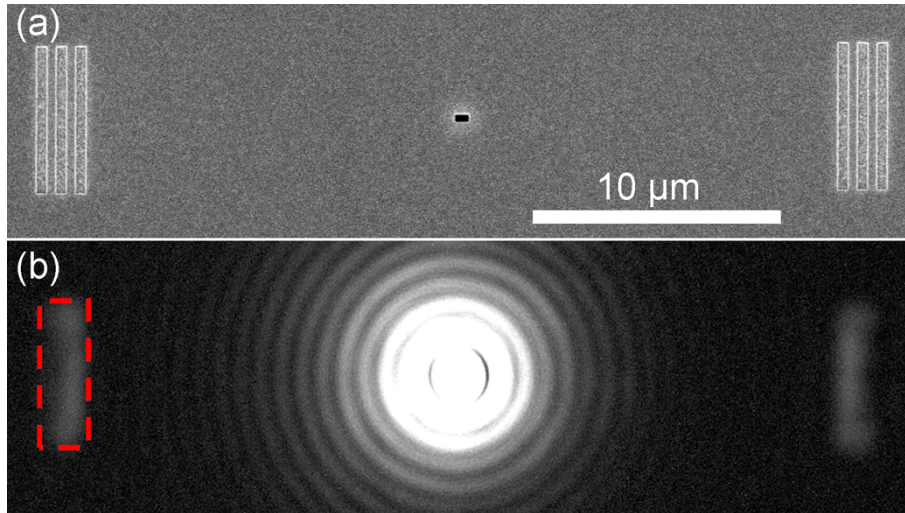


Figure S6. One shortened slit without the coupling plasmonic waveguide. (a) SEM image of the shortened slit structure of about $w=550$ nm and $L=280$ nm, which is not coupled with a plasmonic waveguide. The two decoupling gratings on both sides are used to scatter the generated SPPs. (b) CCD pictures of the scattered light from the experimental sample in Figure S6 (a) at $\lambda=790$ nm. The red dashed rectangle indicates the decoupling grating.